JAMA Neurology | Original Investigation

Assessing Synaptic Density in Alzheimer Disease With Synaptic Vesicle Glycoprotein 2A Positron Emission Tomographic Imaging

Ming-Kai Chen, MD, PhD; Adam P. Mecca, MD, PhD; Mika Naganawa, PhD; Sjoerd J. Finnema, PhD; Takuya Toyonaga, MD, PhD; Shu-fei Lin, PhD; Soheila Najafzadeh, MS; Jim Ropchan, PhD; Yihuan Lu, PhD; Julia W. McDonald, BA; Hannah R. Michalak, BA; Nabeel B. Nabulsi, PhD; Amy F. T. Arnsten, PhD; Yiyun Huang, PhD; Richard E. Carson, PhD; Christopher H. van Dyck, MD

IMPORTANCE Synaptic loss is well established as the major structural correlate of cognitive impairment in Alzheimer disease (AD). The ability to measure synaptic density in vivo could accelerate the development of disease-modifying treatments for AD. Synaptic vesicle glycoprotein 2A is an essential vesicle membrane protein expressed in virtually all synapses and could serve as a suitable target for synaptic density.

OBJECTIVE To compare hippocampal synaptic vesicle glycoprotein 2A (SV2A) binding in participants with AD and cognitively normal participants using positron emission tomographic (PET) imaging.

DESIGN, SETTING, AND PARTICIPANTS This cross-sectional study recruited 10 participants with AD and 11 participants who were cognitively normal between November 2015 and June 2017. We hypothesized a reduction in hippocampal SV2A binding in AD, based on the early degeneration of entorhinal cortical cell projections to the hippocampus (via the perforant path) and hippocampal SV2A reductions that had been observed in postmortem studies. Participants underwent high-resolution PET scanning with ((*R*)-1-((3-(11C-methyl-11C)pyridin-4-yl)methyl)-4-(3,4,5-trifluorophenyl)pyrrolidin-2-one), a compound more commonly known as ^{11}C-UCB-J, for SV2A. They also underwent high-resolution PET scanning with carbon 11–labeled Pittsburgh Compound B (^{11}C-PiB) for β-amyloid, magnetic resonance imaging, and cognitive and neurologic evaluation.

MAIN OUTCOMES AND MEASURES Outcomes were ^{11}C-UCB-J–specific binding (binding potential [BP_{ND}]) via PET imaging in brain regions of interest in participants with AD and participants who were cognitively normal.

RESULTS Ten participants with AD (5 male and 5 female; mean [SD] age, 72.7 [6.3] years; 10 [100%] β-amyloid positive) were compared with 11 participants who were cognitively normal (5 male and 6 female; mean [SD] age, 72.9 [8.7] years; 11 [100%] β-amyloid negative). Participants with AD spanned the disease stages from amnestic mild cognitive impairment (n = 5) to mild dementia (n = 5). Participants with AD had significant reduction in hippocampal SV2A specific binding (41%) compared with cognitively normal participants, as assessed by ^{11}C-UCB-J-PET BP_{ND} (cognitively normal participants: mean [SD] BP_{ND}, 1.47 [0.37]; participants with AD: 0.87 [0.50]; P = .005). These reductions remained significant after correction for atrophy (ie, partial volume correction; participants who were cognitively normal: mean [SD], 2.71 [0.46]; participants with AD: 2.15 [0.55]; P = .02). Hippocampal SV2A-specific binding BP_{ND} was correlated with a composite episodic memory score in the overall sample (R = 0.56; P = .01).

CONCLUSIONS AND RELEVANCE To our knowledge, this is the first study to investigate synaptic density in vivo in AD using ^{11}C-UCB-J–PET imaging. This approach may provide a direct measure of synaptic density, and it therefore holds promise as an in vivo biomarker for AD and as an outcome measure for trials of disease-modifying therapies, particularly those targeted at the preservation and restoration of synapses.

JAMA Neurol. 2018;75(10):1215-1224. doi:10.1001/jamaneurol.2018.1836
Published online July 16, 2018.

Editorial page 1181

Supplemental content

Author Affiliations: Department of Radiology and Biomedical Imaging, Yale University School of Medicine, New Haven, Connecticut (Chen, Naganawa, Finnema, Toyonaga, Lin, Najafzadeh, Ropchan, Lu, Nabulsi, Huang, Carson); Department of Psychiatry, Yale University School of Medicine, New Haven, Connecticut (Mecca, McDonald, Michalak, Arnsten, van Dyck).

Corresponding Author: Ming-Kai Chen, MD, PhD, Department of Radiology & Biomedical Imaging, Yale University School of Medicine, 333 Cedar St, PO Box 208042, New Haven, CT 06520-8042 (ming-kai.chen@yale.edu).

Alzheimer disease (AD) affects 5.5 million people in the United States, and that number is expected to double by 2050 if no cure is identified.[1] From a diagnostic perspective, AD is increasingly viewed along a continuum from preclinical AD to mild cognitive impairment (MCI) to AD dementia.[2] The clinical features of AD are coupled to a distinct pathology, including β-amyloid plaques, neurofibrillary tangles, and synaptic loss.[3] Synapses are crucial for cognitive function, and synaptic loss is a robust and consistent pathology in AD.[4,5] Cognitive impairment in AD is closely correlated with synaptic loss in the association cortex and limbic system.[6,7] Synaptic damage associated with toxic β-amyloid oligomers is observed in the earliest clinical stages of AD,[8] with patients with MCI demonstrating a loss of synapses and synaptic proteins.[4,9-13] Thus the ability to assess synaptic density in vivo would greatly enhance clinical research in AD and would specifically provide a valuable biomarker outcome for therapeutic trials.

Positron emission tomography (PET) imaging is widely used in AD studies to measure glucose metabolism (fluorine 18–fluorodeoxyglucose [^{18}F-FDG]), β-amyloid, and neurofibrillary tangles.[14] Clinically, ^{18}F-FDG-PET imaging is used to differentiate AD from frontotemporal dementia and to track neuronal or synaptic activity as a surrogate biomarker of disease progression.[15] However, ^{18}F-FDG is not a direct biomarker of synaptic density, and test results may be confounded by sensory stimulation, medications, and blood glucose level.[16-19] Inadequate fasting can result in false-positive results in AD scans.[17,18] For this reason, new molecular targets for PET imaging are needed to specifically monitor synaptic density. Synaptic vesicle glycoprotein 2 (SV2) is an essential vesicle membrane protein and could be a suitable target. One of its isoforms, SV2A, is ubiquitously expressed in virtually all synapses.[20-22] Hence, SV2A-PET imaging could provide a highly useful indicator of synaptic density in AD and other neuropsychiatric disorders.

As described in our recent publications,[23-25] ((*R*)-1-((3-(^{11}C-methyl-^{11}C)pyridin-4-yl)methyl)-4-(3,4,5-trifluorophenyl)pyrrolidin-2-one), more commonly known as ^{11}C-UCB-J, has demonstrated excellent characteristics for quantitative SV2A imaging in vivo in both nonhuman primates and humans, with excellent test-retest reproducibility.[25] Excellent correlations were also found among in vivo SV2A-PET measures, in vitro protein expression of SV2A and synaptophysin, a widely used presynaptic marker for synaptic density, and in vitro SV2A binding data in nonhuman primate brain homogenates.[24] Here we report what is, to our knowledge, the first study of in vivo SV2A-PET imaging for quantitative assessment of synaptic density in AD using ^{11}C-UCB-J and high-resolution PET. We hypothesized a reduction in hippocampal binding based on early degeneration of entorhinal cortical cell projections to the hippocampus (via the perforant path)[26,27] and hippocampal SV2A reductions observed in postmortem studies of individuals with AD.[28]

Key Points

Question Can we measure synaptic loss in Alzheimer disease in vivo using positron emission tomography (PET) with the specific radioligand ^{11}C-UCB-J?

Findings This cross-sectional PET imaging study examined ^{11}C-UCB-J–specific binding as a biomarker for synaptic density in 11 cognitively normal elderly participants and 10 participants with mild cognitive impairment to early Alzheimer disease. Significant reductions of hippocampal synaptic densities were found in participants with Alzheimer disease compared with age-matched participants who were cognitively normal.

Meaning PET scanning with ^{11}C-UCB-J may provide a direct measure of synaptic density in Alzheimer disease in vivo; it yields results consistent with previous neuropathological investigations.

Methods

Study Design and Participants

Potentially eligible participants who either had amnestic MCI or mild AD dementia or were cognitively normal and were aged between 55 and 90 years old underwent a screening diagnostic evaluation to ensure eligibility. Participants with AD dementia were required to meet diagnostic criteria for probable dementia because of AD according to the National Institute on Aging-Alzheimer Association[29] and have a Clinical Dementia Rating (CDR) score of 0.5 to 1.0 points and a Mini-Mental State Examination (MMSE) score of 16 to 26 points, inclusive. Participants with MCI were required to meet research diagnostic criteria for amnestic MCI[30] and have a CDR score of 0.5 points and an MMSE score of 24 to 30 points. Both participants with AD dementia and participants with MCI were required to have impaired episodic memory as evidenced by a Logical Memory II (LMII) score of 1.5 SDs less than an education-adjusted norm. Participants who were cognitively normal were required to have a CDR score of 0, an MMSE score greater than 26, and a normal education-adjusted LMII score. The Rey Auditory Verbal Learning Test was also administered to generate an episodic memory score. All participants received a carbon 11–Pittsburgh Compound B (^{11}C-PiB)-PET scan to determine the presence of β-amyloid accumulation. The ^{11}C-PiB-PET scans were considered β-amyloid positive if both visual and quantitative criteria were met. Visual criteria entailed the consensus of 2 experienced readers (M.-K.C. and A.P.M.), and quantitative criteria required a ^{11}C-PiB cerebral-to-cerebellar distribution volume ratio of 1.40 or more in at least 1 AD-affected region of interest (ROI).[31] Consequently, 1 participant with dementia devoid of β-amyloid accumulation and 1 participant who was cognitively normal with positive β-amyloid accumulation were excluded from the study.

The study protocol was approved by the Human Investigation Committee and Radiation Safety Committee at Yale University. All participants provided written informed consent prior to participating in the study.

PET Imaging Experiments

We synthesized ^{11}C-UCB-J per previously described procedures.[23] All participants received 1 dynamic ^{11}C-UCB-J-PET scan on the High Resolution Research Tomograph (Siemens) with a reconstructed image resolution of approximately 3 mm. All PET imaging was performed according to

previously described procedures.[25] All participants also received T1-weighted magnetic resonance images (MRIs) on a 3-T whole-body scanner (Trio; Siemens) for coregistration with the PET images.

Quantitative Analysis

Kinetic analysis was performed voxel by voxel using the 1-tissue compartment (1TC) model[25] and the metabolite-corrected arterial plasma curve to generate a parametric image of distribution volume (V_T). Distribution volume (V_T) is the tissue-to-plasma concentration ratio at equilibrium and reflects total uptake (specific plus nonspecific binding) and is independent of local blood flow change. Images of the delivery rate constant, K_1, which is indicative of perfusion, were also produced. Multiple ROIs were applied to the parametric images using the combined transformations from template to PET space (eMethods in the Supplement). Binding potential (BP_{ND}), a measure of specific binding only, was calculated for each ROI, using the centrum semiovale as the reference region ($BP_{ND} = V_{T\,ROI} / V_{Treference} - 1$).

We also applied the simplified reference tissue model 2 (SRTM2)[32] using the centrum semiovale as a reference region to estimate regional-specific binding (BP_{ND}) without use of the arterial input function (eMethods in the Supplement). To evaluate the contributions of atrophy to the PET outcome measures, we masked ROIs with a segmented MRI (gray matter mask) and performed partial volume correction (PVC) according to previously described procedures.[33] In addition to the primary ROI analysis, voxelwise analysis was performed on K_1, V_T, and BP_{ND} images for comparison between AD and cognitively normal groups using Statistical Parametric Mapping version 12 (SPM12; Wellcome Trust Centre for Neuroimaging). We also performed MRI volumetric analysis of cortical and subcortical gray matter volumes between AD and cognitively normal groups using FreeSurfer version 6 (Massachusetts General Hospital).[34,35]

Statistical Analysis

Statistical calculations were performed using SPSS version 24 (IBM) and PRISM version 7 (GraphPad). Comparison of mean total uptake (V_T) and specific binding (BP_{ND}) values in the hippocampus between AD and cognitively normal groups was performed with 2-tailed, unpaired *t* test with $P < .05$ as a threshold for significance. A linear mixed model was also used to explore ^{11}C-UCB-J binding in multiple regions (within-participant factor) between the cognitively normal and AD groups. Additional exploratory analyses examined the relationship between hippocampal-specific binding (BP_{ND}) and episodic memory (average of *z* scores for LMII and the Rey Auditory Verbal Learning Test) and global function (CDR sum of boxes [CDR-SB]) in the combined sample with Pearson correlation coefficients, 2-tailed, with $P < .05$ as a threshold for significance.

Results

Twenty-one participants, including 10 with amnestic MCI due to AD or mild AD dementia and 11 who were cognitively normal, completed the study between November 2015 and June 2017. One PiB-negative participant with dementia and 1 PiB-positive participant who was cognitively normal were excluded. As shown in **Table 1**, the diagnostic groups were well balanced for age, sex, and education, and both groups were highly educated (with a mean [SD] of 16.9 [2.8] years in the group with AD and 17.3 [2.4] years of education in the cognitively normal group). The mean (SD) age of the group with AD was 72.7 (6.3) years and that of the cognitively normal group was 72.9 (8.7) years. The participants with AD had clinical characteristics typical of amnestic MCI and mild AD dementia, with a mean (SD) MMSE score of 24.1 (4.8) points and a mean (SD) CDR-global score of 0.75 (0.26) points.

Table 1. Demographic Information and Test Results of Included Participants

Characteristic	No. (%)	
	Cognitively Normal Participants	Participants With Alzheimer Disease
Total participants	11	10
With mild Alzheimer disease	NA	5 (50)
With mild cognitive impairment	NA	5 (50)
Sex		
Male	5 (45)	5 (50)
Female	6 (55)	5 (50)
Age, mean (SD) [range], y	72.9 (8.7) [61.2-82.7]	72.7 (6.3) [63.1-82.9]
Education, mean (SD) [range], y	17.3 (2.4) [12-20]	16.9 (2.8) [12-20]
CDR-global, mean (SD) [range]	0 (0) [NA]	0.75 (0.26) [0.5-1]
CDR-SB, mean (SD) [range]	0 (0) [NA]	4.3 (2.6) [0.5-9.0]
MMSE, mean (SD) [range]	29.3 (1.2) [27-30]	24.1 (4.8) [17-29]
LMII, mean (SD) [range]	14.6 (2.9) [8-18]	1.7 (2.8) [0-7]
RAVLT-delay, mean (SD) [range]	11.6 (3.2) [4-15]	1.3 (2.4) [0-7]

Abbreviations: CDR-global, Clinical Dementia Rating global score; CDR-SB, Clinical Dementia Rating–sum of boxes; LMII, Logical Memory II score; MMSE, Mini-Mental State Examination; NA, not applicable; RAVLT, Rey Auditory Verbal Learning Test.

All participants received 1 injection of ^{11}C-UCB-J (mean [SD] quantity, 493 [224] MBq), with no significant difference in radioactivity or mass dose between groups. The arterial input functions were successfully measured in 9 participants with AD and 8 participants who were cognitively normal, enabling kinetic analysis with the 1TC model to estimate V_T, BP_{ND}, and K_1. Consistent with our hypothesis, ^{11}C-UCB-J binding was significantly reduced in the hippocampus of participants with AD compared with participants who were cognitively normal, suggesting loss of SV2A and synaptic density in this region (**Figure 1**; **Table 2**). The V_T in the hippocampus was 28% lower in participants with AD (participants with AD: mean [SD], 8.85 [2.58] mL/cm^3; participants who were cognitively normal: 12.27 [2.26] mL/cm^3; $P = .01$). Importantly, V_T values of the white matter centrum semiovale were virtually identical between the groups (Table 2), supporting its suitability for use as a reference region. A reduction in BP_{ND} of 44% was found in the hippocampus of participants with AD (participants with AD: mean

Figure 1. Representative Total Uptake (V_T) Parametric Synaptic Vesicle Glycoprotein 2A Positron Emission Tomographic (PET) Images

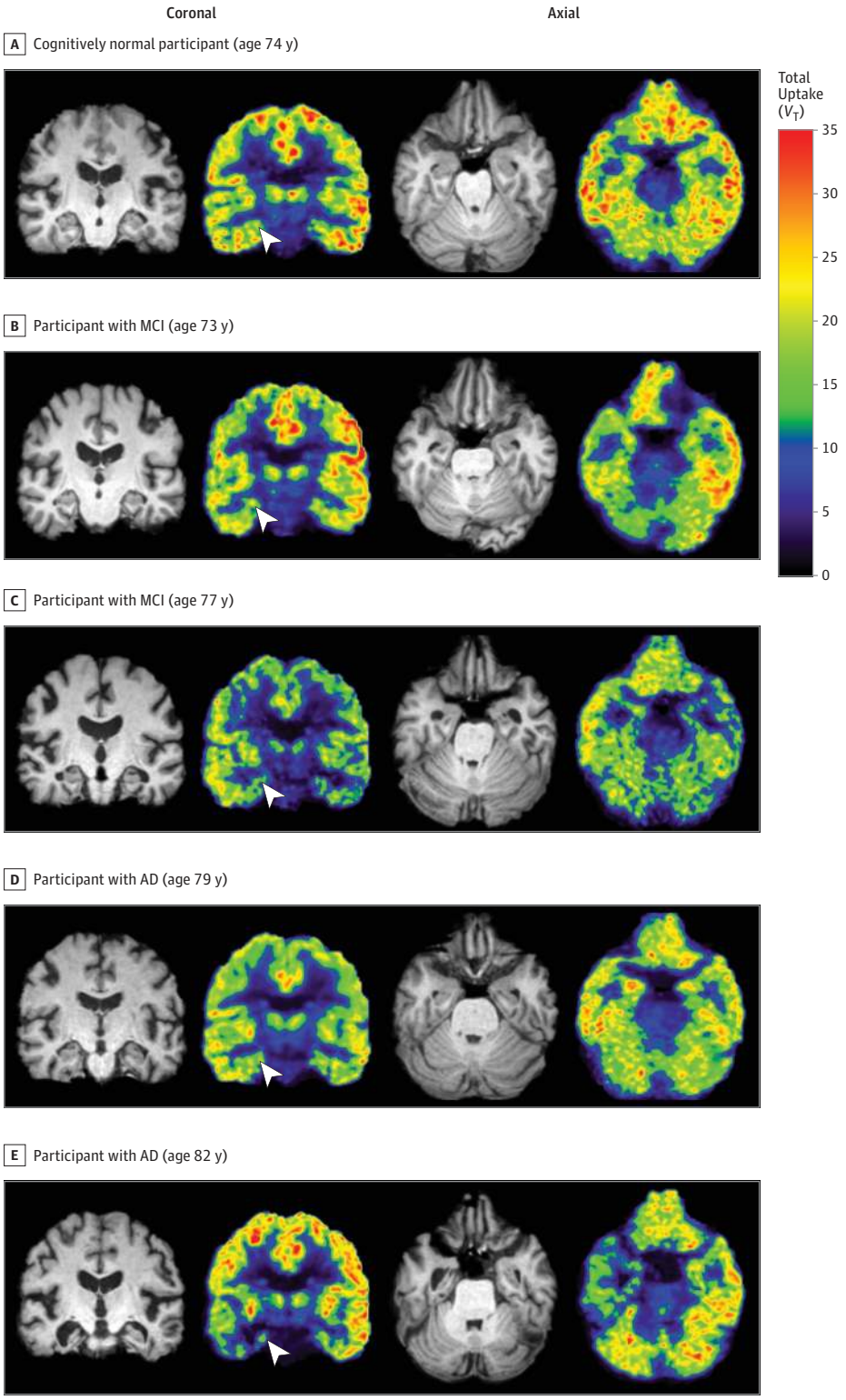

Representative coronal and axial images of parametric ^{11}C-UCB-J–PET scans (V_T) and magnetic resonance imaging scans in participants who were cognitively normal (A), participants with mild cognitive impairment (MCI) (B and C), and mild Alzheimer disease (AD) dementia (D and E). The cognitively normal participant had a negative carbon 11–labeled Pittsburgh Compound B (^{11}C-PiB) scan, and all participants with AD had positive ^{11}C-PiB–PET scans. The pseudocolor in PET images represents the intensity of ^{11}C UCB-J binding (V_T). Evident reduction of ^{11}C-UCB-J binding in the hippocampus of participants with AD was noted compared with participants who were cognitively normal (the arrowhead denotes the right hippocampus). Various degrees of reduction can be visualized in the temporoparietal cortex of the participant with MCI (B and C), the right temporoparietal cortex of the participant with mild AD dementia (D), and the right temporal cortex of participant E. MCI indicates mild cognitive impairment.

[SD], 0.87 [0.59]; participants who were cognitively normal: 1.54 [0.29]; P = .01; Table 2). The addition of age as a covariate in these statistical models did not improve the goodness of fit or alter the results.

An exploratory analysis of multiple ROIs was performed using a linear mixed model and showed a significant diagnostic group-region interaction for both V_T ($F_{11,187}$ = 2.6; P = .004) and BP_{ND} ($F_{11,187}$ = 2.7; P = .003). This analysis suggested ad-

Table 2. Synaptic Vesicle Glycoprotein 2A Positron Emission Tomography Outcome Measures in Brain Regions of Interest[a]

Region of Interest	V_T, mL/cm^3			BP_{ND}		
	Mean (SD)			Mean (SD)		
	Cognitively Normal Participants (n = 8)	Participants With AD (n = 9)	*P* Value	Cognitively Normal Participants (n = 8)	Participants With AD (n = 9)	*P* Value
Primary region						
Hippocampus	12.27 (2.26)	8.85 (2.58)	.01	1.54 (0.29)	0.87 (0.59)	.01
Exploratory regions						
Caudate nucleus	12.98 (4.04)	11.90 (3.06)	.54	1.65 (0.51)	1.50 (0.63)	.60
Cerebellum	12.98 (1.71)	13.14 (1.47)	.84	1.69 (0.21)	1.76 (0.31)	.61
Cingulate gyrus, anterior	17.61 (1.71)	17.48 (2.59)	.91	2.66 (0.17)	2.67 (0.50)	.95
Cingulate gyrus, posterior	13.48 (1.12)	12.45 (2.13)	.24	1.82 (0.32)	1.60 (0.40)	.24
Entorhinal cortex	14.85 (2.49)	11.96 (2.36)	.03	2.07 (0.23)	1.52 (0.54)	.02
Frontal cortex	17.19 (2.14)	16.86 (2.66)	.78	2.56 (0.18)	2.52 (0.40)	.80
Occipital cortex	17.42 (2.12)	16.94 (2.61)	.69	2.62 (0.26)	2.56 (0.58)	.82
Parietal cortex	17.81 (1.97)	17.15 (2.73)	.58	2.70 (0.23)	2.60 (0.59)	.67
Pulvinar nucleus	14.21 (2.30)	11.77 (2.29)	.04	1.94 (0.24)	1.49 (0.57)	.06
Putamen	20.10 (2.03)	20.74 (2.51)	.58	3.17 (0.16)	3.35 (0.40)	.28
Temporal cortex	18.27 (2.37)	16.96 (2.24)	.26	2.79 (0.20)	2.56 (0.50)	.26
Thalamus	13.01 (2.43)	11.30 (2.07)	.14	1.68 (0.23)	1.38 (0.49)	.13
Reference region						
Centrum semiovale	4.82 (0.54)	4.78 (0.51)	.88	NA	NA	NA

Abbreviations: AD, Alzheimer disease; BP_{ND}, binding potential (specific binding) of ^{11}C-UCB-J in brain regions of interest; NA, not applicable; V_T, volume of distribution (total brain uptake).

[a] *P* values are for 2-tailed, unpaired *t* tests. Results for exploratory regions used post hoc comparisons (uncorrected for multiplicity) from a linear mixed-model analysis of PET measures in multiple regions (within-participant factor) between cognitively normal and AD groups; significant results were found for diagnostic group-region interaction for V_T ($F_{11,187}$ = 2.6; P = .004) and BP_{ND} ($F_{11,187}$ = 2.7; P = .003).

ditional significant reductions of SV2A V_T in participants with AD in both the entorhinal cortex (participants with AD: mean [SD], 11.96 [2.36] mL/cm^3; participants who were cognitively normal: 14.85 [2.49] mL/cm^3; P = .03) and the pulvinar nucleus (participants with AD: mean [SD], 11.77 [2.29] mL/cm^3; participants who were cognitively normal: 14.21 [2.30] mL/cm^3; P = .04), uncorrected for multiple comparisons (Table 2).

To better illustrate the regional reduction of SV2A in the brain, SPM analysis was performed with surface rendering of differences in V_T and K_1 between participants with AD (n = 9) and participants who were cognitively normal (n = 8). **Figure 2**A shows a significant reduction of SV2A binding in the hippocampus of participants with AD. Figure 2B presents group differences in the delivery rate constant K_1, which extend to the temporal lobe, parietal lobe, and posterior cingulate gyrus in addition to the hippocampus. Notably, the patterns of SV2A V_T for synaptic density and K_1 differed in individual participants (Figure 1; eFigure 2 in the Supplement). The region-of-interest analysis of K_1 (eTable 1 in the Supplement) did not show statistically significant reductions in temporal or parietal cortices, likely attributable to a diluted effect in larger ROIs. Notably, the pattern of regional K_1 reduction in the participant with AD, reflecting reduced cerebral blood flow, was thus similar to that of hypometabolism in AD, as demonstrated by ^{18}F-FDG-PET scan.

Because arterial data were not available for 1 participant with AD and 3 participants who were cognitively normal, SRTM2 was used to analyze the entire cohort. The value of hippocampal-specific binding BP_{ND} generated by this method was highly correlated with that obtained from the 1TC model with the arterial input function (R^2 = 0.95; P < .001; eFigure 1 in the Supplement). Using SRTM2 in the full cohort, hippocampal BP_{ND} was reduced by 41% in participants with AD (n = 10) compared with participants who were cognitively normal (n = 11) (participants with AD: mean [SD], 0.87 [0.50]; participants who were cognitively normal: 1.47 [0.37]; P = .005; **Figure 3**A).

To evaluate the contribution of gray matter tissue loss to SV2A reductions in participants with AD, we performed gray matter masking and PVC. The reduction in hippocampal SV2A binding in participants with AD remained significant with gray matter masking with respect to 1TC-derived V_T (participants with AD: mean [SD], 11.4 [2.2]; participants who were cognitively normal: 14.0 [2.0]; P = .02), BP_{ND} (participants with AD: mean [SD], 1.39 [0.50]; participants who were cognitively normal: 1.91 [0.24]; P = .02), and SRTM2-derived BP_{ND} (participants with AD: mean [SD], 1.35 [0.42]; participants who were cognitively normal: 1.85 [0.39]; P = .01). The reduction in hippocampal SV2A binding was nonsignificant after PVC with respect to 1TC-derived V_T (participants with AD: mean [SD], 15.5 [3.0]; participants who were cognitively normal: 18.4 [2.8]; P = .06) and BP_{ND} (participants with AD: mean [SD], 2.26 [0.66]; participants who

Figure 2. Voxelwise Analysis of Total Uptake (V_T) and Perfusion (K_1) With Statistical Parametric Mapping in Participants with Alzheimer Disease (AD) Compared With Cognitively Normal Participants

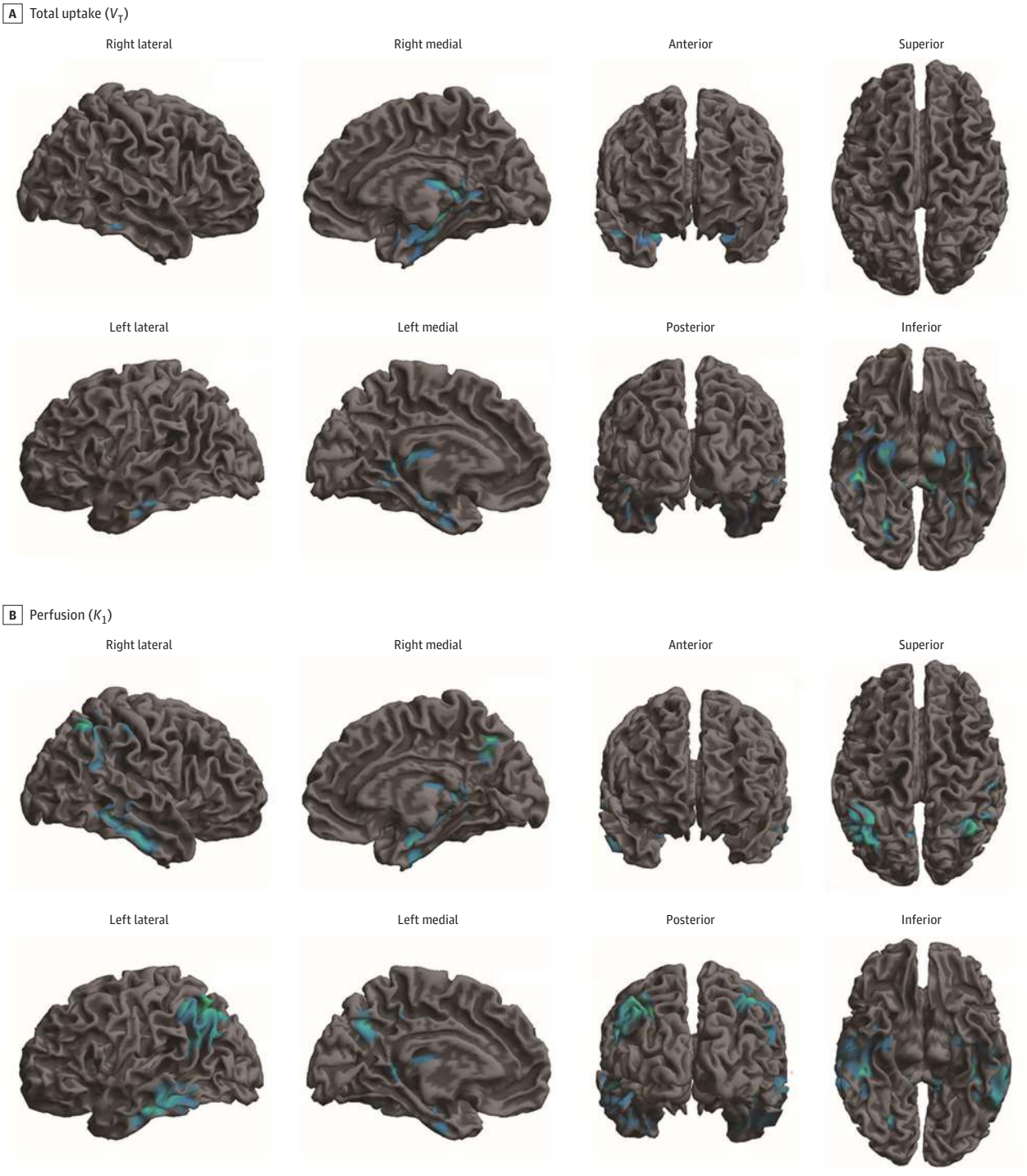

This Figure includes 9 participants with AD and 8 cognitively normal participants. A, Blue indicates the regions with statistically significant reduction of V_T in participants with AD compared with those who were cognitively normal, rendered on brain surfaces at different projections. The statistically significant reduction of ^{11}C-UCB-J binding in the hippocampus was consistent with the findings from region-of-interest analysis. B, Blue indicates a statistically significant reduction of K_1 in the participant with AD compared with the cognitively normal participant. A broader regional reduction of K_1 emerged in the temporoparietal cortices in the participant with AD.

were cognitively normal: 2.81 [0.34]; P = .05) but remained significant with respect to SRTM2-derived BP_{ND} (participants with AD: mean [SD], 2.15 [0.55]; participants who were cognitively normal: 2.71 [0.46]; P = .02) (eFigure 3 in the Supplement).

Figure 3. Comparison of Hippocampal Binding Potential (BP_{ND}) From Simplified Reference Tissue Model 2 (SRTM2) and Correlation With Clinical Findings

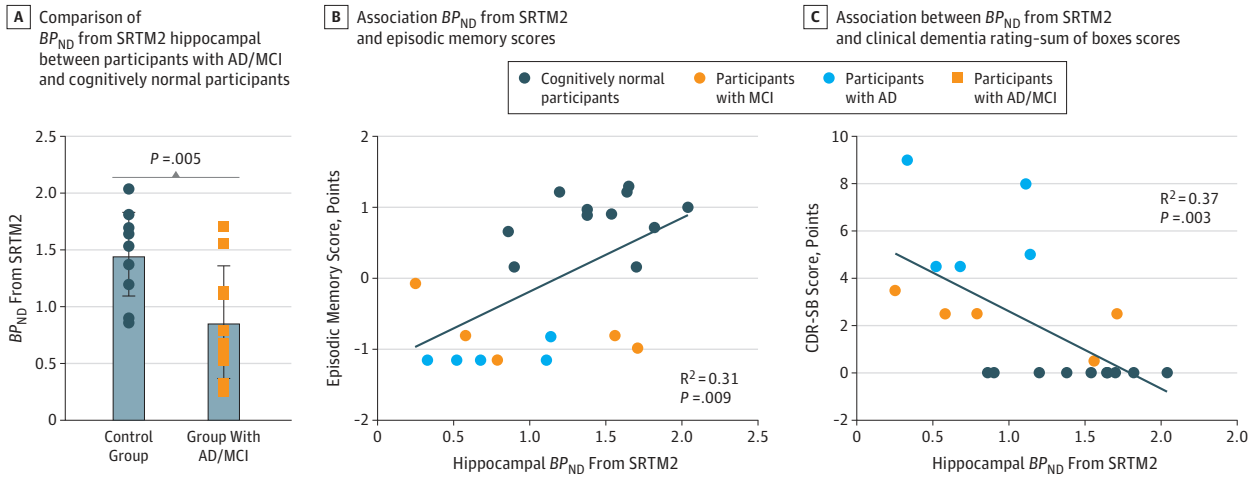

A, Comparison of BP_{ND} from SRTM2 in the hippocampus between participants with Alzheimer disease (AD) and cognitively normal participants. Error bars represent standard deviations. MCI indicates mild cognitive impairment. B, Association between hippocampal BP_{ND} from SRTM2 and episodic memory scores. A statistically significant correlation was observed between BP_{ND} in the hippocampus and an episodic memory score. C, Association between hippocampal BP_{ND} from SRTM2 and Clinical Dementia Rating-sum of boxes (CDR-SB) score.

The exploratory reduction in SV2A binding in the entorhinal cortex (Table 2) did not withstand PVC with respect to 1TC-derived V_T (participants with AD: mean [SD], 21.2 [4.3]; participants who were cognitively normal: 22.7 [4.2]; P = .48), BP_{ND} (participants with AD: mean [SD], 3.44 [0.89]; participants who were cognitively normal: 3.67 [0.54]; P = .54; eTable 2 in the Supplement), which was consistent with the profound early atrophy that has been found to occur in this region.[26] In fact, MRI volumetric analysis demonstrated an approximate 25% reduction in the entorhinal cortex of participants with AD compared with participants who are cognitively normal (participants with AD: mean [SD] gray matter volume, 2.3 [0.4]; participants who were cognitively normal: 2.9 [0.6] cm^3; P = .01; eTable 3 in the Supplement), which was similar to the approximate 27% reduction of BP_{ND} in the entorhinal cortex of participants with AD (participants with AD: mean [SD], 1.52 [0.54]; participants who were cognitively normal: 2.07 [0.23]; P = .02; Table 2). However, there was only a 22% reduction of hippocampal volume of participants with AD compared with participants who were cognitively normal (participants with AD: mean [SD] volume, 6.0 [0.9]; participants who were cognitively normal: 7.4 [1.0] cm^3; P = .003) (eTable 3 in the Supplement), which was much less than the 44% reduction of 1TC-derived hippocampal BP_{ND} in participants with AD (participants with AD: mean [SD] BP_{ND}, 0.87 [0.59]; participants who were cognitively normal: 1.54 [0.29]; P = .01; Table 2). Therefore, the loss of hippocampal SV2A-specific BP_{ND} in participants with AD was much greater than the degree of brain atrophy.

Pearson correlations were performed to assess the relationship between synaptic density estimated by SV2A binding and clinical assessments (Figure 3). Statistically significant correlations were found between SRTM2-derived hippocampus BP_{ND} and episodic memory (based on mean z scores from the LMII and Rey Auditory Verbal Learning Test; R = 0.56; P = .01) and SRTM2-derived hippocampus BP_{ND} and the CDR-SB score (R = −0.61; P = .003). Notably, 2 participants with MCI had relatively high and outlying values for hippocampal BP_{ND}.

Discussion

Synaptic loss in the association cortex and limbic system is a robust and consistent pathology in AD[4] and is closely correlated with cognitive impairment.[6,7] However, until now, the assessment of synaptic density and the quantification of presynaptic proteins in AD could only be performed in postmortem brain tissues. The present study demonstrated, for the first time, that noninvasive PET imaging with ^{11}C-UCB-J is capable of measuring reductions in synaptic density in vivo in the hippocampus of individuals with amnestic MCI and mild AD dementia. This finding was established by ROI analysis and corroborated by an exploratory whole-brain, voxel-wise analysis. The potential applications of SV2A-PET imaging with ^{11}C-UCB-J as an in vivo biomarker in AD include the early detection of synaptic loss, the monitoring of disease progression, and the evaluation of synaptic rescue and recovery through therapeutic interventions.

Considerable postmortem and brain biopsy research has been devoted to the characterization of synaptic loss in AD. Most of these studies have necessarily been conducted in patients with advanced dementia.[4] However, some postmortem work[9-11,13,36] has been performed in patients at the prodromal AD or MCI stages. Because these studies vary by stage of disease and the early-stage studies frequently involve single brain regions, we presently lack a cohesive map of regional synaptic loss in early-stage AD.

Postmortem work has established rather unequivocally that the earliest significant degeneration in AD occurs in en-

torhinal cortical cells.[26,27] Compared with control participants, individuals with mild AD have been demonstrated to have a 60% reduction in cell count in layer II and 40% reduction in layer IV of the entorhinal cortex.[26] Since these cells project via the perforant path to all fields of the hippocampal formation, including the dentate gyrus, Cornu Ammonis (CA) fields, and the subiculum, we expected that the earliest and largest reductions in SV2A binding would be in the hippocampus. Indeed, pathology studies have reported a reduction in synapses in the outer molecular layer of dentate gyrus of 44% in mild AD and 13% to 20% in MCI,[10,13] as well as a reduction of 55% in patients with mild AD and 18% in patients with MCI in the CA1 field.[9] These postmortem findings are consistent with the reductions in SV2A binding observed in the present study, in vivo, with ^{11}C-UCB-J-PET, as measured by BP_{ND} (41%). Notably, the only study to our knowledge that measured SV2A (and synaptophysin) in postmortem brain samples of individuals with AD also revealed reductions in the hippocampus.[28]

The fact that our exploratory analysis of multiple brain regions found reduced SV2A binding in the entorhinal cortex is not unexpected, because degenerating entorhinal cortical cells also have local projections. However, the reduced SV2A binding in the entorhinal cortex may reflect the profound early atrophy in this region,[26] as this reduction, unlike those in the hippocampus, was almost identical to the degree of volume loss (eTable 3 in the Supplement) and did not persist after PVC. This is consistent with a postmortem study of synaptic density in MCI that found no reductions in the entorhinal cortex.[13] On the other hand, the fact that this exploratory analysis did not reveal synaptic losses in other brain regions, including the association cortical regions, may be attributable to limited statistical power in this small and disproportionately early-stage sample. Some,[11,12] but not all,[13,36] pathologic studies of association cortical regions in participants with MCI have shown synaptic reductions. Postmortem samples of individuals with MCI are difficult to recruit, and the participants in the referenced studies are approximately 15 years older (with a mean age of 87 to 89 years[9-12,36]) than those in the present study. Larger samples spanning more disease stages will be needed to provide a more comprehensive mapping of SV2A binding in patients with AD with ^{11}C-UCB-J-PET imaging. However, we expect that the largest losses in early-stage AD will continue to be observed in the hippocampus. As suggested by our data, possible SV2A decreases in the pulvinar nucleus may also be seen in early-stage AD,[37] perhaps reflecting the loss of axon terminals from the association cortices (eFigure 4 in the Supplement). However, this will require a larger cohort for confirmation.

The results of our exploratory K_1 parametric imaging, which reflects blood flow, are very similar to the classic pattern of ^{18}F-FDG-PET in AD,[15] with decreased glucose metabolism or synaptic activity in the temporoparietal cortices. We propose that K_1 parametric imaging with ^{11}C-UCB-J may serve as a surrogate for brain perfusion, because similar concepts have been investigated previously using the early dynamic images with PET amyloid tracers.[38-40] We plan to compare K_1 parametric imaging from ^{11}C-UCB-J-PET scans with ^{18}F-FDG-PET imaging in the same participants to evaluate the usefulness of K_1 imaging in the clinical setting. This feature may yield useful information about perfusion or synaptic activity from K_1 mapping of early images and synaptic density from V_T or BP_{ND} parametric images within a single ^{11}C-UCB-J-PET study.

Limitations

Whether SV2A binding in AD is a direct measure of synaptic density is unclear. DeKosky and Scheff[7] reported that, in frontal cortical biopsy specimens of patients with AD, synaptic contact size increased and may have compensated for the numerical loss of synapses. Moreover, Snow et al[41] have described an accumulation of SV2A in dystrophic neurites within the neuritic plaques, which might obscure synaptic loss in amyloid-rich regions.

In the combined samples of individuals who were cognitively normal and individuals with AD, we also observed statistically significant correlations between hippocampal SV2A specific binding (BP_{ND}) with both episodic memory score and global functioning (CDR-SB). The degree of association was only moderate, attributable in part to 2 participants with MCI who had outlying higher hippocampal SV2A binding. Interestingly, those 2 participants also had only minimal hippocampal atrophy on MRI scan. Larger samples are needed to clarify cognitive associations with regional SV2A binding in AD samples. Longitudinal within-participants analyses may be more powerful in this regard.

Conclusions

In conclusion, we have demonstrated, to our knowledge for the first time, reduced synaptic density in the hippocampus of living people with AD by PET imaging of SV2A with the radioligand ^{11}C-UCB-J. This method provides a direct measure of SV2A and synaptic density and therefore holds promise as a novel in vivo biomarker for AD and an outcome measure for trials of disease-modifying therapies, particularly those that target the preservation and restoration of synapses. Our novel SV2A-PET imaging for quantifying synaptic density in vivo could also provide a very useful and noninvasive tool for clinical and translational studies in a wide variety of neurologic and psychiatric disorders.

ARTICLE INFORMATION

Accepted for Publication: May 4, 2018.

Published Online: July 16, 2018.
doi:10.1001/jamaneurol.2018.1836

Author Contributions: Dr Chen had full access to all of the data in the study and takes responsibility for the integrity of the data and the accuracy of the data analysis.
Study concept and design: Chen, Mecca, Carson, van Dyck.
Acquisition, analysis, or interpretation of data: Chen, Mecca, Ropchan, Naganawa, Finnema, Toyonaga, Lin, Najafzadeh, Lu, McDonald, Michalak, Nabulsi, Arnsten, Huang, Carson, van Dyck.
Drafting of the manuscript: Chen, Mecca,

Naganawa, Toyonaga, Lin, Arnsten, Carson, van Dyck.
Critical revision of the manuscript for important intellectual content: Chen, Mecca, Finnema, Ropchan, Lu, McDonald, Michalak, Nabulsi, Najafzadeh, Arnsten, Huang, Carson, van Dyck.
Statistical analysis: Chen, Mecca, Naganawa, Toyonaga, Lin, Lu, Carson, van Dyck.
Obtained funding: Chen, Mecca, Carson, van Dyck.
Administrative, technical, or material support: Chen, Mecca, Naganawa, Lin, Najafzadeh, McDonald, Michalak, Nabulsi, Huang, van Dyck.
Study supervision: Chen, Lin, Ropchan, Nabulsi, Carson, van Dyck.

Conflict of Interest Disclosures: Dr Chen reports research support from the Dana Foundation and research support from Eli Lilly and clinical trials from Merck, outside the submitted work. Dr Huang reports research grants from the UCB and Eli Lilly outside the submitted work. Drs Huang and Carson have a patent for a newer version of the tracer pending. Dr Carson reports grants from National Institutes of Health for the conduct of the study. Dr Carson also reports having received grants from AstraZeneca, Astellas, Eli Lilly, Pfizer, Taisho, and UCB, outside the submitted work. Dr van Dyck reports consulting fees from Kyowa Kirin, Roche, Merck, Eli Lilly, and Janssen and grants for clinical trials from Biogen, Novartis, Eli Lilly, Merck, Eisai, Janssen, Roche, Genentech, Toyama, and TauRx, outside the submitted work. No other disclosures are reported.

Funding/Support: The study was supported by The Dana Foundation David Mahoney Neuroimaging Grant (Dr Chen), a pilot grant from Yale Alzheimer's Disease Research Center (via National Institutes of Health grant P50AG047270, Dr Chen), and National Institutes of Health grant R01AG52560-01A1 (Drs Carson and van Dyck). Dr Finnema was supported by an international postdoctoral grant from the Swedish Research Council.

Role of the Funder/Sponsor: The funders had no role in the design and conduct of the study; collection, management, analysis, and interpretation of the data; preparation, review, or approval of the manuscript; and decision to submit the manuscript for publication.

Additional Contributions: We thank all study participants and staff persons from the Yale Alzheimer's Disease Research Unit for recruiting and evaluating participants and from the Yale PET Center for their expert assistance in conducting the PET studies. We also thank UCB Pharma for providing the radiolabeling precursor and reference standard. No compensation was provided from study funders for these contributions.

REFERENCES

1. Alzheimer's Association. 2017 Alzheimer's disease facts and figures. *Alzheimers Dement*. 2017;13(4):325-373. doi:10.1016/j.jalz.2017.02.001

2. Jack CR Jr, Albert MS, Knopman DS, et al. Introduction to the recommendations from the National Institute on Aging-Alzheimer's Association workgroups on diagnostic guidelines for Alzheimer's disease. *Alzheimers Dement*. 2011;7(3):257-262. doi:10.1016/j.jalz.2011.03.004

3. Overk CR, Masliah E. Pathogenesis of synaptic degeneration in Alzheimer's disease and Lewy body disease. *Biochem Pharmacol*. 2014;88(4):508-516. doi:10.1016/j.bcp.2014.01.015

4. Scheff SW, Neltner JH, Nelson PT. Is synaptic loss a unique hallmark of Alzheimer's disease? *Biochem Pharmacol*. 2014;88(4):517-528. doi:10.1016/j.bcp.2013.12.028

5. Selkoe DJ. Alzheimer's disease is a synaptic failure. *Science*. 2002;298(5594):789-791. doi:10.1126/science.1074069

6. Terry RD, Masliah E, Salmon DP, et al. Physical basis of cognitive alterations in Alzheimer's disease: synapse loss is the major correlate of cognitive impairment. *Ann Neurol*. 1991;30(4):572-580. doi:10.1002/ana.410300410

7. DeKosky ST, Scheff SW. Synapse loss in frontal cortex biopsies in Alzheimer's disease: correlation with cognitive severity. *Ann Neurol*. 1990;27(5):457-464. doi:10.1002/ana.410270502

8. Pham E, Crews L, Ubhi K, et al. Progressive accumulation of amyloid-beta oligomers in Alzheimer's disease and in amyloid precursor protein transgenic mice is accompanied by selective alterations in synaptic scaffold proteins. *FEBS J*. 2010;277(14):3051-3067. doi:10.1111/j.1742-4658.2010.07719.x

9. Scheff SW, Price DA, Schmitt FA, DeKosky ST, Mufson EJ. Synaptic alterations in CA1 in mild Alzheimer disease and mild cognitive impairment. *Neurology*. 2007;68(18):1501-1508. doi:10.1212/01.wnl.0000260698.46517.8f

10. Scheff SW, Price DA, Schmitt FA, Mufson EJ. Hippocampal synaptic loss in early Alzheimer's disease and mild cognitive impairment. *Neurobiol Aging*. 2006;27(10):1372-1384. doi:10.1016/j.neurobiolaging.2005.09.012

11. Scheff SW, Price DA, Schmitt FA, Scheff MA, Mufson EJ. Synaptic loss in the inferior temporal gyrus in mild cognitive impairment and Alzheimer's disease. *J Alzheimers Dis*. 2011;24(3):547-557. doi:10.3233/JAD-2011-101782

12. Scheff SW, Price DA, Ansari MA, et al. Synaptic change in the posterior cingulate gyrus in the progression of Alzheimer's disease. *J Alzheimers Dis*. 2015;43(3):1073-1090.

13. Masliah E, Mallory M, Hansen L, DeTeresa R, Alford M, Terry R. Synaptic and neuritic alterations during the progression of Alzheimer's disease. *Neurosci Lett*. 1994;174(1):67-72. doi:10.1016/0304-3940(94)90121-X

14. McKhann GM, Knopman DS, Chertkow H, et al. The diagnosis of dementia due to Alzheimer's disease: recommendations from the National Institute on Aging-Alzheimer's Association workgroups on diagnostic guidelines for Alzheimer's disease. *Alzheimers Dement*. 2011;7(3):263-269. doi:10.1016/j.jalz.2011.03.005

15. Landau SM, Harvey D, Madison CM, et al; Alzheimer's Disease Neuroimaging Initiative. Associations between cognitive, functional, and FDG-PET measures of decline in AD and MCI. *Neurobiol Aging*. 2011;32(7):1207-1218. doi:10.1016/j.neurobiolaging.2009.07.002

16. Wiers CE, Shokri-Kojori E, Wong CT, et al. Cannabis abusers show hypofrontality and blunted brain responses to a stimulant challenge in females but not in males. *Neuropsychopharmacology*. 2016;41(10):2596-2605. doi:10.1038/npp.2016.67

17. Ishibashi K, Onishi A, Fujiwara Y, Ishiwata K, Ishii K. Relationship between Alzheimer disease-like pattern of 18F-FDG and fasting plasma glucose levels in cognitively normal volunteers. *J Nucl Med*. 2015;56(2):229-233. doi:10.2967/jnumed.114.150045

18. Burns CM, Chen K, Kaszniak AW, et al. Higher serum glucose levels are associated with cerebral hypometabolism in Alzheimer regions. *Neurology*. 2013;80(17):1557-1564. doi:10.1212/WNL.0b013e31828f17de

19. Teipel SJ, Drzezga A, Bartenstein P, Möller HJ, Schwaiger M, Hampel H. Effects of donepezil on cortical metabolic response to activation during (18)FDG-PET in Alzheimer's disease: a double-blind cross-over trial. *Psychopharmacology (Berl)*. 2006;187(1):86-94. doi:10.1007/s00213-006-0408-1

20. Bajjalieh SM, Frantz GD, Weimann JM, McConnell SK, Scheller RH. Differential expression of synaptic vesicle protein 2 (SV2) isoforms. *J Neurosci*. 1994;14(9):5223-5235. doi:10.1523/JNEUROSCI.14-09-05223.1994

21. Bajjalieh SM, Peterson K, Linial M, Scheller RH. Brain contains two forms of synaptic vesicle protein 2. *Proc Natl Acad Sci U S A*. 1993;90(6):2150-2154. doi:10.1073/pnas.90.6.2150

22. Janz R, Südhof TC. SV2C is a synaptic vesicle protein with an unusually restricted localization: anatomy of a synaptic vesicle protein family. *Neuroscience*. 1999;94(4):1279-1290. doi:10.1016/S0306-4522(99)00370-X

23. Nabulsi NB, Mercier J, Holden D, et al. Synthesis and preclinical evaluation of 11C-UCB-J as a PET tracer for imaging the synaptic vesicle glycoprotein 2A in the brain. *J Nucl Med*. 2016;57(5):777-784. doi:10.2967/jnumed.115.168179

24. Finnema SJ, Nabulsi NB, Eid T, et al. Imaging synaptic density in the living human brain. *Sci Transl Med*. 2016;8(348):348ra96. doi:10.1126/scitranslmed.aaf6667

25. Finnema SJ, Nabulsi NB, Mercier J, et al. Kinetic evaluation and test-retest reproducibility of [^{11}C]UCB-J, a novel radioligand for positron emission tomography imaging of synaptic vesicle glycoprotein 2A in humans [published online January 1, 2017]. *J Cereb Blood Flow Metab*. doi:10.1177/0271678X17724947.

26. Gómez-Isla T, Price JL, McKeel DW Jr, Morris JC, Growdon JH, Hyman BT. Profound loss of layer II entorhinal cortex neurons occurs in very mild Alzheimer's disease. *J Neurosci*. 1996;16(14):4491-4500. doi:10.1523/JNEUROSCI.16-14-04491.1996

27. Braak H, Thal DR, Ghebremedhin E, Del Tredici K. Stages of the pathologic process in Alzheimer disease: age categories from 1 to 100 years. *J Neuropathol Exp Neurol*. 2011;70(11):960-969. doi:10.1097/NEN.0b013e318232a379

28. Robinson JL, Molina-Porcel L, Corrada MM, et al. Perforant path synaptic loss correlates with cognitive impairment and Alzheimer's disease in the oldest-old. *Brain*. 2014;137(pt 9):2578-2587. doi:10.1093/brain/awu190

29. Jack CR Jr, Knopman DS, Weigand SD, et al. An operational approach to National Institute on Aging-Alzheimer's Association criteria for preclinical Alzheimer disease. *Ann Neurol*. 2012;71(6):765-775. doi:10.1002/ana.22628

30. Albert MS, DeKosky ST, Dickson D, et al. The diagnosis of mild cognitive impairment due to Alzheimer's disease: recommendations from the National Institute on Aging-Alzheimer's Association workgroups on diagnostic guidelines for Alzheimer's disease. *Alzheimers Dement*. 2011;7(3):270-279. doi:10.1016/j.jalz.2011.03.008

31. Reiman EM, Chen K, Liu X, et al. Fibrillar amyloid-beta burden in cognitively normal people at 3 levels of genetic risk for Alzheimer's disease. *Proc Natl Acad Sci U S A*. 2009;106(16):6820-6825. doi:10.1073/pnas.0900345106

32. Wu Y, Carson RE. Noise reduction in the simplified reference tissue model for neuroreceptor functional imaging. *J Cereb Blood Flow Metab*. 2002;22(12):1440-1452. doi:10.1097/01.WCB.0000033967.83623.34

33. Mecca AP, Barcelos NM, Wang S, et al. Cortical β-amyloid burden, gray matter, and memory in adults at varying APOE ε4 risk for Alzheimer's disease. *Neurobiol Aging*. 2018;61:207-214. doi:10.1016/j.neurobiolaging.2017.09.027

34. Buckner RL, Head D, Parker J, et al. A unified approach for morphometric and functional data analysis in young, old, and demented adults using automated atlas-based head size normalization: reliability and validation against manual measurement of total intracranial volume. *Neuroimage*. 2004;23(2):724-738. doi:10.1016/j.neuroimage.2004.06.018

35. Fischl B. FreeSurfer. *Neuroimage*. 2012;62(2):774-781. doi:10.1016/j.neuroimage.2012.01.021

36. Scheff SW, Price DA, Schmitt FA, Roberts KN, Ikonomovic MD, Mufson EJ. Synapse stability in the precuneus early in the progression of Alzheimer's disease. *J Alzheimers Dis*. 2013;35(3):599-609.

37. Kuljis RO. Lesions in the pulvinar in patients with Alzheimer's disease. *J Neuropathol Exp Neurol*. 1994;53(2):202-211. doi:10.1097/00005072-199403000-00012

38. Meyer PT, Hellwig S, Amtage F, et al. Dual-biomarker imaging of regional cerebral amyloid load and neuronal activity in dementia with PET and 11C-labeled Pittsburgh compound B. *J Nucl Med*. 2011;52(3):393-400. doi:10.2967/jnumed.110.083683

39. Kadir A, Almkvist O, Forsberg A, et al. Dynamic changes in PET amyloid and FDG imaging at different stages of Alzheimer's disease. *Neurobiol Aging*. 2012;33(1):198.e1-198.e14. doi:10.1016/j.neurobiolaging.2010.06.015

40. Rodriguez-Vieitez E, Carter SF, Chiotis K, et al. Comparison of early-phase 11c-deuterium -l-deprenyl and 11c-pittsburgh compound b pet for assessing brain perfusion in Alzheimer disease. *J Nucl Med*. 2016;57(7):1071-1077. doi:10.2967/jnumed.115.168732

41. Snow AD, Nochlin D, Sekiguichi R, Carlson SS. Identification in immunolocalization of a new class of proteoglycan (keratan sulfate) to the neuritic plaques of Alzheimer's disease. *Exp Neurol*. 1996;138(2):305-317. doi:10.1006/exnr.1996.0069